UDC 624 . 014 . 27 : 693 . 814 . 2

Beam-to-Column Connections Using High-Strength Blind Bolts and Their Applications in Actual Buildings

Masahiro NAGATA*(1) Yasumi SHIMURA*(1)
Nobuyoshi UNO*(2) Hiroshi TANAKA*(2)

Abstract:

A welded joint system using diaphragm plates is generally applied to the beam-to-column connections of moment-resisting frames that are configured with the square tube columns and wide flange beams frequently used for steel structures. These connections are structurally very important to assure earthquake resistance in frames, which are the most highly fabricated parts of steel structures and require strict quality control because of many spots to be welded. The examples of disaster in the Kobe Earthquake have even made it important to control the quality of spot-welds on columns with beams. This report describes a new bolted joint system "the hyper-frame system" which has obtained general approval of the Ministry of Construction. The hyper-frame system uses newly developed high-strength blind bolts which provide the capability of clamping closed sections such as square tube columns.

1. Introduction

The hyper-frame system shown in **Fig. 1** is a steel structure of moment-resisting frames which use cold formed square tubes (BCR295) for the columns and rolled wide flange (SN400B) for the beams. The combinations are limited to the range shown in **Table 1**. The beam-to-column connections are semi-rigid joints without the diaphragm plate that has been used in conventional joint systems. The T-stub (rolled CT sections, SN490B) tensile joint with the use of torque-control, high-strength blind bolt[1,2] (hereinafter TCBB) enables clamping against closed sections. Also the column joint can be used as a double-shear friction joint when necessary.

While assembly by the conventional joint system shown in **Fig. 2(a)** requires a lot of welding, the new joint system in **Fig. 2(b)**, necessitates only making bolt openings for the T-stub joints and no cutoffs of square tube columns to set up the diaphragm plate, groove processing and welding. Although the new joint system needs to have precise bolt openings, no inspection or control of high-grade welding techniques or welding quality is necessary and the work involves only bolt clamping with machine tools. The system ensures consistent and stable work quality. Significant productivity improvement in fabrication process is also possible.

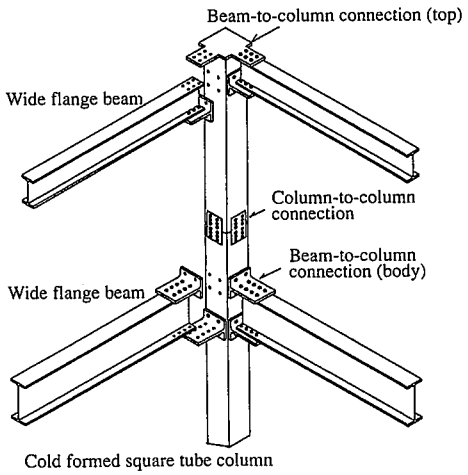

Fig. 1 Outline of hyper-frame system

*(1) Construction & Architectural Materials Development & Engineering Service Div.
*(2) Technical Develometn Bureau

Table. 1 Applied range and used members of hyper-frame system

Applied range

Member	Material	Size	Remarks
Column	Cold formed square tube BCR295	□-250×12 - □-400×22	
Beam	Hot-rolled wide flange SN400B	H-250×125×6/9 - H-488×300×11/18	JIS size
		H-400×200×9/12 - H-600×200×9/19	Hyper-beam

Used members

Joint members	Material
T-stub	Hot rolled CT section (SN490B)
High-strength bolt for tension joint	Torque-control, high-strength blind bolt (TCBB) HUCK International, Inc.
High-strength bolt for friction joint	Torque-control, high-strength bolt for friction bolt joint (S10T)

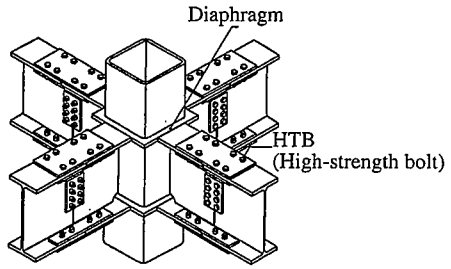

Fig. 2(a) Conventional joint system

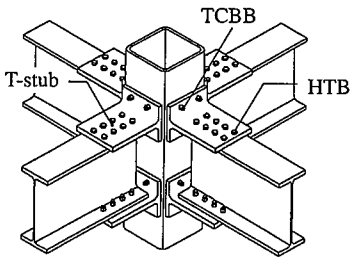

Fig. 2(b) New joint system

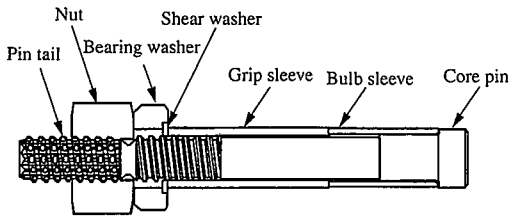

Fig. 3 Torque-control, high-strength blind bolt (TCBB)

2. Behavior of Connections using TCBB

2.1 TCBB

TCBB used in this system is made up of 6 components: core pin, bulb sleeve, grip sleeve, shear washer, bearing washer and nut shown in **Fig. 3**. The TCBB clamping procedure is shown in **Photo 1**. The bolt is inserted from one side of the connection, the nut is rotated with an electric shear wrench, the bulb sleeve has buckling formations to make bolt heads (special washers) and finally, the pin tail is split to complete clamping from only one direction. Two kinds of TCBB are prepared: TCBB 24 with nominal diameter 24 mm and TCBB 27 with nominal diameter 27 mm. The test results will be introduced mainly using TCBB 24.

2.1.1 Tensile test of materials

Table 2 shows the tensile test results of the sub-size test piece JIS No. 4 (round bar test piece 10 mm in diameter) which is cut out from the TCBB 24 pins. The tensile strength is slightly over the upper limit of JIS (120 kgf/mm²) for F10T high-strength bolts, but the elongation after fracture or restriction are equivalent to F10T.

2.1.2 Mechanical properties of bolt sets

Regarding the bolt set (TCBB 24, clamping thickness 70 mm) after applying tension, **Fig. 4** shows the relationship between the load and the strain of bolt heads in a simple tensile test and cyclic tensile test which use a punching jig. The load is supposed to be a clearance load when strain at the bolt head greatly changes in the simple tensile test of Fig. 4(a), the applied tension is about 21 tons and the fracture load is about 29 tons. The fracture of the bolts occurs at the threaded portion and this shows that the punched strength at the bolt heads which did buckle at the bulb sleeves is more than

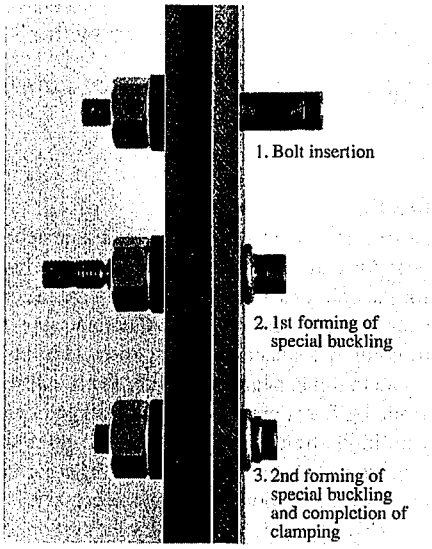

Photo 1 Clamping procedures of TCBB

Table 2 Tensile test results of TCBB 24

Test No.	0.2% offset strength (kgf/mm²)	Tensile strength (kgf/mm²)	Uniform elongation (%)	Elongation after fracture (%)	Reduction of area (%)
N1	114.6	122.4	6.0	18.3	56.9
N2	111.9	123.4	6.0	18.5	59.3
N3	114.6	122.0	6.0	18.5	59.0
Average	113.7	122.6	6.0	18.4	58.4

the fracture strength at the bolt axial portion. The repetitive test results in Fig. 4(b) also show stable quality without deteriorating bolt heads or diminished withstand load performance.

Fig. 5 shows the relaxation test results of TCBB 24 with clamping thickness 35 mm. The striking decrease of the bolt tension cannot be observed, so TCBB 24 has relaxation characteristics equivalent to ordinary high-strength bolts. Based on these results, the design bolt tension, allowable stress and so on were decided as shown in **Table 3**[3].

2.2 Behavior of connections

2.2.1 Simple T-stub tensile tests

T-stub tensile tests were conducted as shown in **Fig. 6**, using CT sections cut out from rolled wide flange (H-900 × 300 × 16/28). Four kinds of test specimens were used as shown in **Table 4**, with the bolt types (high-strength bolts of F8T-M24 for the comparison with TCBB 24, HTB hereinafter) and bolt numbers as the experiment variables.

Fig. 7 shows the load-deformation curve. Although the stiffness after the yield strength of the test specimen using TCBB 24 (TT-4 and TT-8) is lower than that of the test specimen using HTB (TH-4 and TH-8), it is clear that the T-stub connections using TCBB 24 have proof stress equivalent to HTB in terms of both yield strength and the maximum proof stress. After clamping TCBB 24, the grip sleeve is not involved in force transmission and the tension applied into the bolts is transmitted only through the pins. The cause of the decreased stiffness is that the actual section area of this pin is smaller than that of F8T-M24-HTB with equivalent strength. The design bolt tensions of TCBB 24 and F8T-M24-HTB are both about 19 tons and the yield stress values ($_cP4_y$, $_cP8_y$) are, according to the calculation results according to the evaluation formula of "Standard for Limit State Design of Steel Structures (draft)[4]" for a T-stub joint of 4 bolts and 8 bolts, 658 and 1,040 kN respectively, and the maximum strength

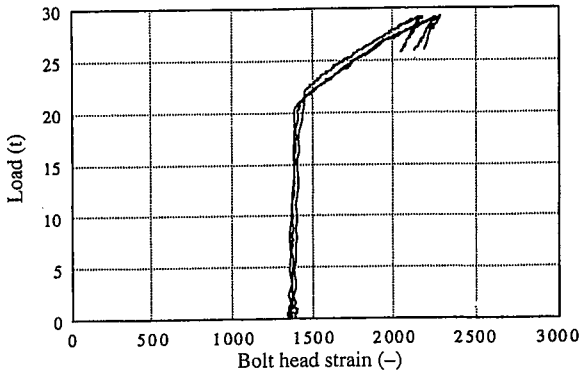

(a) Monotonic loading

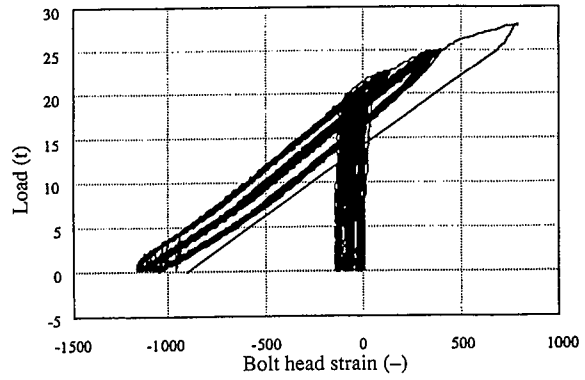

(b) Cyclic loading

Fig. 4 Tensile test results of bolt sets after clamping

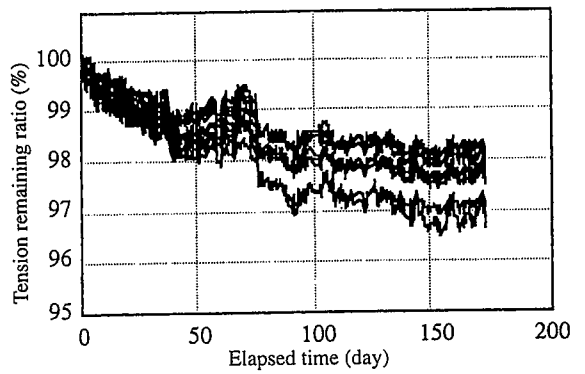

Fig. 5 Relaxation test results

Table 3 Design values for TCBB

	Bolt size (mm)			Bolt design bearing force (t)		
	Nominal diameter	Actual outside diameter	Installation hole diameter	Design bolt tension	Standard bolt tension	Maximum tensile strength
TCBB24	24	24.5	26.0	18.1	20.0	26.8
TCBB27	27	28.5	30.0	25.9	28.7	38.4

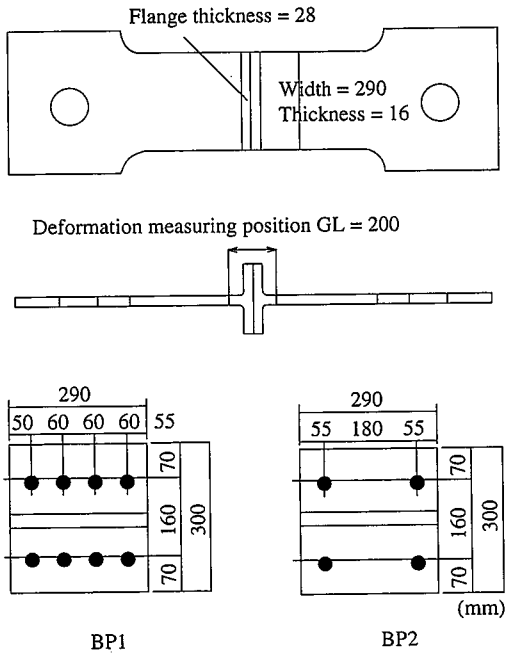

Fig. 6 T-stub tensile test

Table 4 Test specimen list

Name of test body	Type of bolt	Number of bolt	Bolt plan
TT-8	TCBB	8	BP1
TH-8	HTB(F8T)	8	BP1
TT-4	TCBB	4	BP2
TH-4	HTB(F8T)	4	BP2

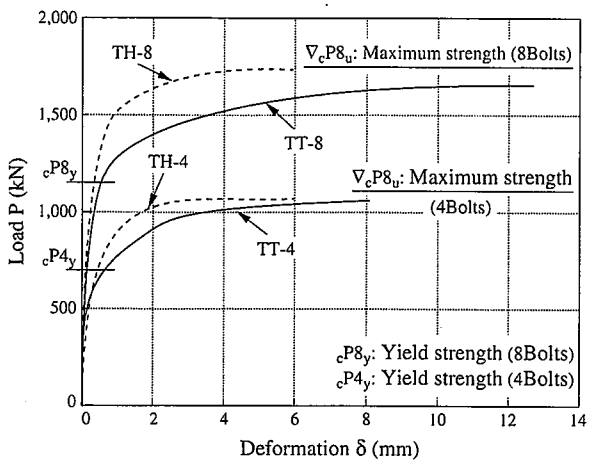

Fig. 7 Load–deformation relationship of T-stub tensile test

($_cP4_u$, $_cP8_u$) are 1,089 and 1,692 kN, which corresponds well with the test results. Furthermore, the increase from 4 to 8 in the number of bolts produces a stress increase 1.6 times the proof stress formula. Therefore, the strength of the T-stub joint using TCBB 24 is, as in the case of using HTB, possible to evaluate with the strength evaluation formula given in the above draft standard.

2.2.2 Tensile test of beam-to-column connections

In order to identify the behavior of beam-to-column connections using TCBB, a partial-model tensile test for the T-stub connections of square tube columns was conducted with the test specimen shape shown in **Fig. 8**. As in the simple T-stub tensile test, the test variables are kinds, number of bolts, the test specimen outline and test results are shown in **Table 5**. The load–deformation relationship is in **Fig. 9**, where JT-4 and JT-8 using TCBB 24 and JH-4 and JH-8 using F8T-M24-HTB have almost the same strength for both 4-bolt and 8-bolt types.

For both TCBB and HTB, the maximum strength of 8 bolts is around 1.2 times as much as that of 4 bolts, which is short of the strength increase rate (1.6 times) in the simple T-stub tensile test. This is because the joint strength is decided by the values of the T-stub strength and the out-of-plane strength of the square tube. As shown in Table 5 the strength of 4-bolt test specimen is decided by the T-stub strength, while that of 8 bolts is determined by the out-of-plane strength of the square tube calculated with the yield line theory, using the model shown in **Fig. 10**[5,6]. This model is only made up of outside bolts, even where 4 bolts are arranged across the width of the square tube (test specimen JT-8 and JH-8). **Fig. 11** shows the strain change in the bolt heads of the outside and inside bolts. While the T-stub tensile test in Fig. 11(a) shows the same behaviors both in outside and inside bolts, the joint tensile test (JT-8) in Fig. 11(b) is different; the outside bolts are mainly resistant and the inside bolts do not contribute to the strength. This shows that this model is appropriate as a strength evaluation model for bolt plans arranged in a row across the width. But the 8-bolt calculated value tends to overestimate the test value slightly (there is no problem with the design in the hyper-frame system, since only the 4-bolt type is used).

2.2.3 Cyclic loading test by cruciform partial framing

A cyclic loading test was conducted using actual-size cruciform partial framing with the test specimen shown in **Fig. 12**. The test specimen outline and test results are given in **Table 6**. The experiment variables are the square tube thickness (12, 16 mm) and the beam size. Also a comparative test was carried out on the welding joint system (D16-450) with a conventional through diaphragm. The

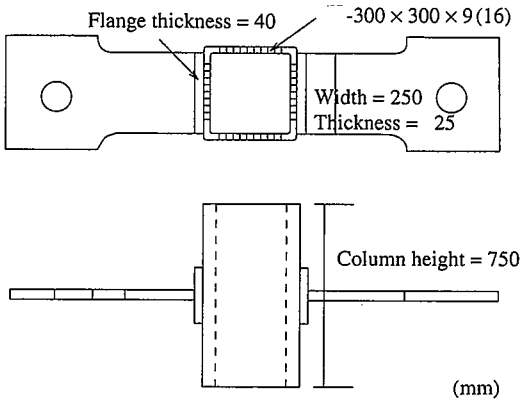

Fig. 8 Test specimen in tensile test on beam-to-column connections

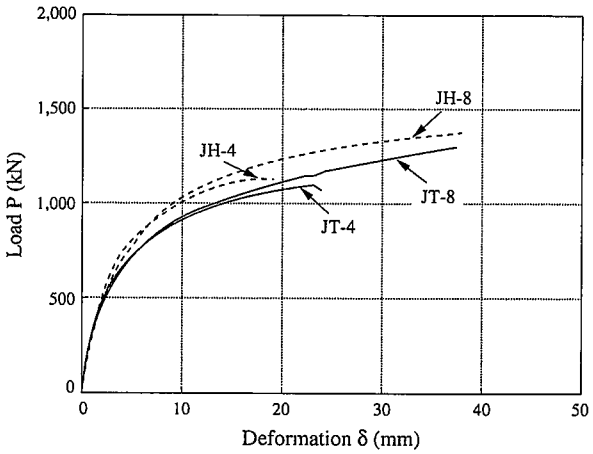

Fig. 9 Tensile test results of beam-to-column connections

Table 5 Outline of beam-to-column connection test specimen and tensile test results

Name of test specimen	Type of bolt	Number of bolt	Bolt plan	Local strength of square tube column skins $_jP$		Maximum strength of T-stub connection $_tP$		Minimum of $_jP$ and $_tP$, $_cP$		Experimental results		$_eP_y/_cP_y$	$_eP_m/_cP_m$
				$_jP_y$(kN)	$_jP_m$(kN)	$_tP_y$(kN)	$_tP_m$(kN)	$_cP_y$(kN)	$_cP_m$(kN)	$_eP_y$(kN)	$_eP_m$(kN)		
JT-8	TCBB	8	BP1	1,240	1,399	1,070	1,692	1,070	1,399	855	1,298	0.80	0.93
JH-8	HTB(F8T)	8	BP1	1,240	1,399	1,070	1,692	1,070	1,399	1,015	1,375	0.95	0.98
JT-4	TCBB	4	BP2	1,240	1,399	701	1,089	701	1,089	753	1,096	1.07	1.01
JH-4	HTB(F8T)	4	BP2	1,240	1,399	701	1,089	701	1,089	785	1,131	1.12	1.04

Note y: Yield strength, m:Maximum strength

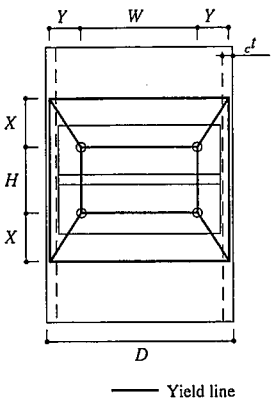

$$ {}_jP_y = 4\,{}_cM_p\left(\frac{2Y+W}{X}+\frac{2X+H}{Y}\right) $$

$$ {}_jP_m = 4\,{}_cM_u\left(\frac{2Y+W}{X}+\frac{2X+H}{Y}\right) $$

$$ X=\sqrt{\frac{(2Y+W)Y}{2}} \qquad Y=\frac{D-{}_ct-W}{2} $$

$$ {}_cM_p=\frac{{}_ct^2\,{}_c\sigma_y}{4} \qquad {}_cM_u=\frac{{}_ct^2\,{}_c\sigma_t}{4} $$

${}_ct$: Thickness of steel pipe
${}_c\sigma_y$: Yield point of steel pipe
${}_c\sigma_t$: Tensile strength of steel pipe

Fig. 10 Out-of-plane deformation of square tube

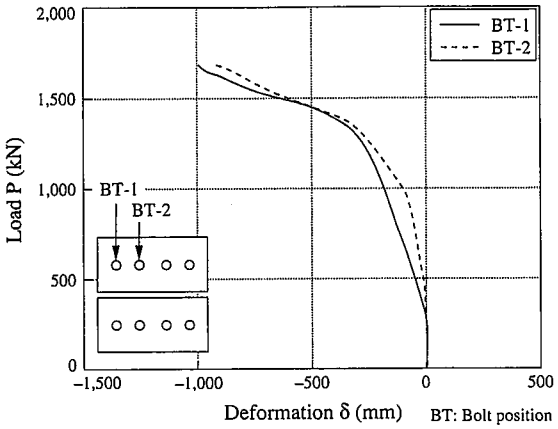

(a) T-stub tensile test (TT-8)

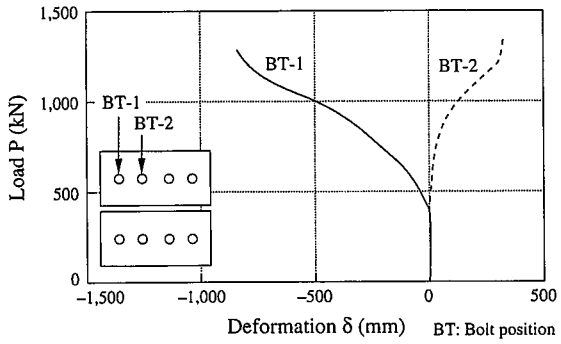

(b) Beam-to-column connection tensile test (JT-8)

Fig. 11 Strain of bolt head

cyclic loading test is conducted by alternate loading at the beam ends as shown in Fig. 8, while a compressive load of 20% of the column yield strength was applied to the column. The loading is done with displacement control and the displacement is increased for every two cycles.

Table 6 shows the ratio α^* to the total plastic moment of beam ${}_bM_p$ of the maximum strength M_m and the plastic deformation ratio $\mu = \theta_{max} / (\theta_p - 1)$ obtained from the skeleton curve, as well as the cumulative plastic deformation ratio $\eta = \Sigma E_{+(-)} / (M_p \cdot \theta_p)$ obtained from the hysteresis curve. **Fig. 13** shows the hysteresis curve on load–deformation at the beam ends.

It is clear that all the test specimen satisfy the full beam plastic moments and possess adequate plastic deformation capability. The test specimen with the new joint system has decreased stiffness after yielding, while D16-450 has such stable hysteresis that each cycle expands the loop. The partial load decline in the hysteresis curve is due to the slip in the friction bolt joint between the T-stub and the beam flange.

In the final state of each test specimen (C12-400 to C16-500) using the new joint system, beam flange buckling in C16-400 can be also observed, but most of these were bolt fractures. The maximum strength was assumed to be decided in each area in the test specimen design stage. However, the reevaluation using the actual values of the mechanical properties of the steel indicated that the maximum strength for all the test specimens is governed by the joint strength. The test results show that the larger the beam height, the greater the maximum strength becomes, because the T-stub and bolts have the same specifications in all the test specimens.

Fig. 14 is a comparison of the skeleton curve in the load–deformation relationship with the test specimens for which the column and beam size are the same in the above cyclic loading test of the

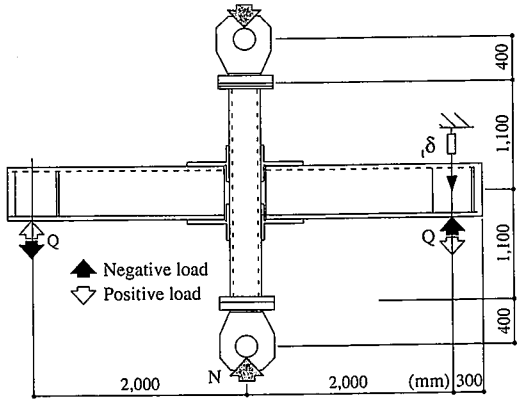

Fig. 12 Cruciform partial frame test

Table 6 Outline of cruciform partial frame test specimen and test results

Test specimen outline			Yield strength(kN·m)		Experimental results (kN·m)				Plastic deformation ratio		Cumulative plastic deformation ratio	
Symbol	Column	Beam	${}_bM_p$	${}_jM_p$	M_m^+	α^*	M_m^-	α^*	μ^+	μ^-	η^+	η^-
C12-400	□-300×12	H-400×200×8/13	420	236	424	1.01	426	1.01	2.04	1.93	17.8	16.3
C16-400	□-300×16	H-400×200×8/13	420	368	579	1.38	612	1.46	3.28	4.06	24.0	21.6
C16-450	□-300×16	H-450×200×9/14	531	413	620	1.17	636	1.20	2.22	2.29	19.3	15.9
C16-500	□-300×16	H-500×200×10/16	634	457	653	1.03	659	1.04	1.49	1.65	14.1	17.0
D16-450	□-300×16	H-450×200×9/14	531	——	668	1.06	660	1.05	3.83	3.10	12.9	14.6

Note ${}_bM_p$: Full plastic moment of the beam, ${}_jM_p$: Joint yield moment, α^*: Ratio of the maximum strength M_m to ${}_bM_p$

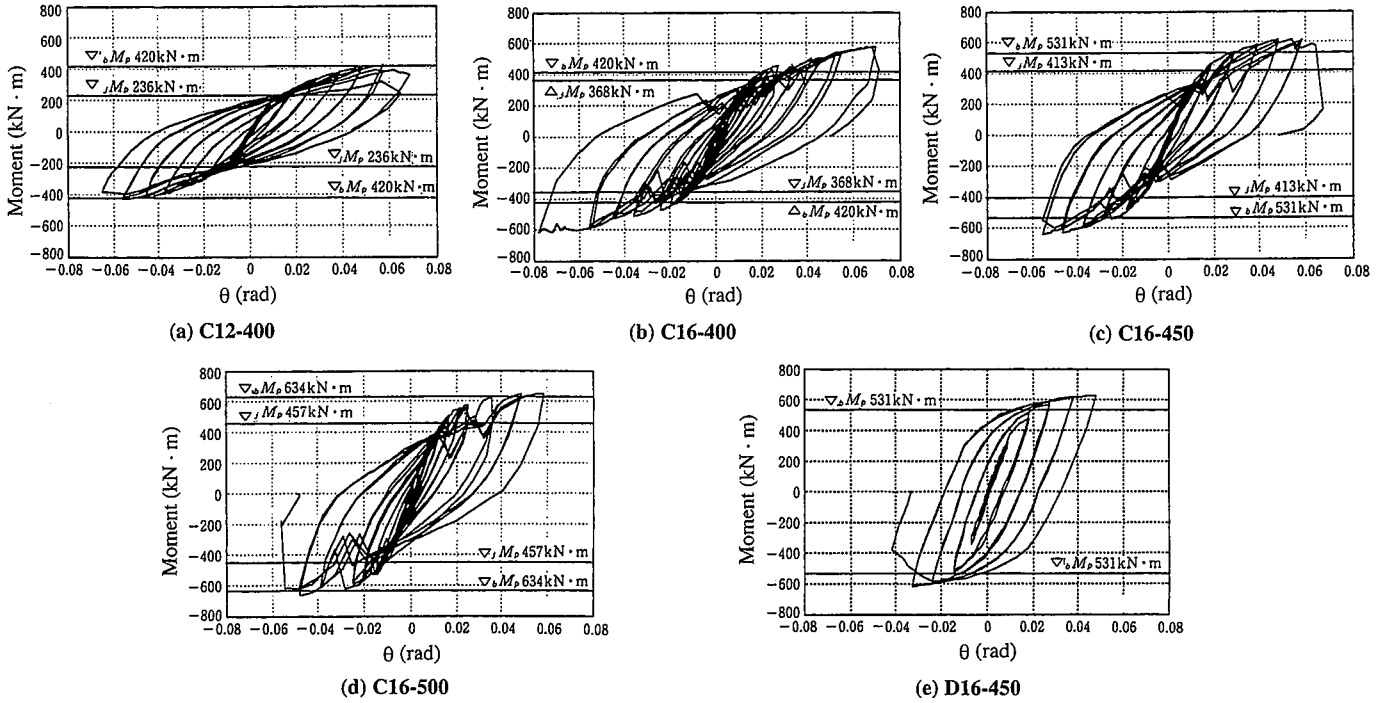

Fig. 13 Moment-rotation relationship under cyclic loading

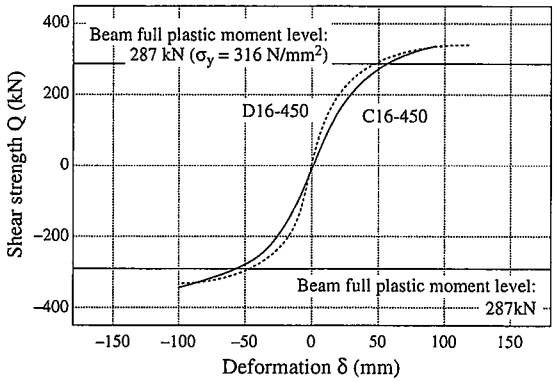

Fig. 14 Effect of the existence of diaphragm

cruciform partial framing to observe the effect the use of the diaphragm has on the frame stiffness. Though the stiffness (C16-450) of the overall frames using the new joint system is about 10 to 15% lower than the welding joint system (D16-450) with a diaphragm plate, but it is not an extreme decline in stiffness.

3. Hyper-Frame System Design

3.1 Design procedures

It is possible to design frames using this system by adding considerations for strength of the T-stub joints of the square tube columns and wide flange beams as well as considerations for story drifts of frames, which allows for the decreased stiffness of the joint for lack of diaphragm plates. But in the Hyper-Frame System Standard Design Manual[7] and for each combination of columns and beams shown in Table 1, various design values for standard details and the allowable strength and the standard joint details are prepared. By utilizing the above design manual for the actual design, the special attention in the joint design can be omitted.

Fig. 15 shows the design flow[8]. In seismic design for severe earthquakes, it is possible to design with route 2 in the A-type joint which satisfies the conditions of retained strength connection. But in the case of mixed use of B-type or C-type joints, the calculation of ultimate lateral shear should be necessary.

3.2 Design in beam-to-column connections

3.2.1 Strength of beam-to-column connections

The yield moment ($_jM_y$) in the square tube and T-stub connections should be the smaller value of either the local strength of square tube column skins ($_cM_y$) or maximum strength of T-stub connection ($_tM_y$).

$$_jM_y = \min.\ (_cM_y,\ _tM_y) \qquad \cdots\cdots (1)$$

Here $_cM_y = {}_cP_y \cdot h$, $_tM_y = {}_tP_y \cdot h$. The local strength of column skins ($_cP_y$) of the square tubes is given in the formula calculated by yield line theory using the model shown in Fig. 10. And for the tensile strength of the T-stub ($_tP_y$), the design formula shown in "Standard for Limit State Design of Steel Structures (draft)" should be applied. The relevancy of both proof stress formulas were evaluated in the confirmation experiment in Sec. 2.2 and the values were converted into beam end moment multiplied by the distance (h) of the center line of the T-stub web attached to the upper and lower flanges of the beam.

The shear force from the beam is transmitted by the friction bolt joint of the T-stub and the square tube columns which will be compressed by bending moment. The compressive force producing the friction should be the larger value, either by the initial clamping force introduced to the bolts or by the axial force caused by beam moment. The shear force from beams in seismic design for severe earthquakes, with no expectation for the friction bolt joint, was confirmed by the bolt shear strength. Moreover, a stress calculation similar to the ordinary connections was conducted for the friction joint of T-stub web and wide flange beams and the panel zones of columns.

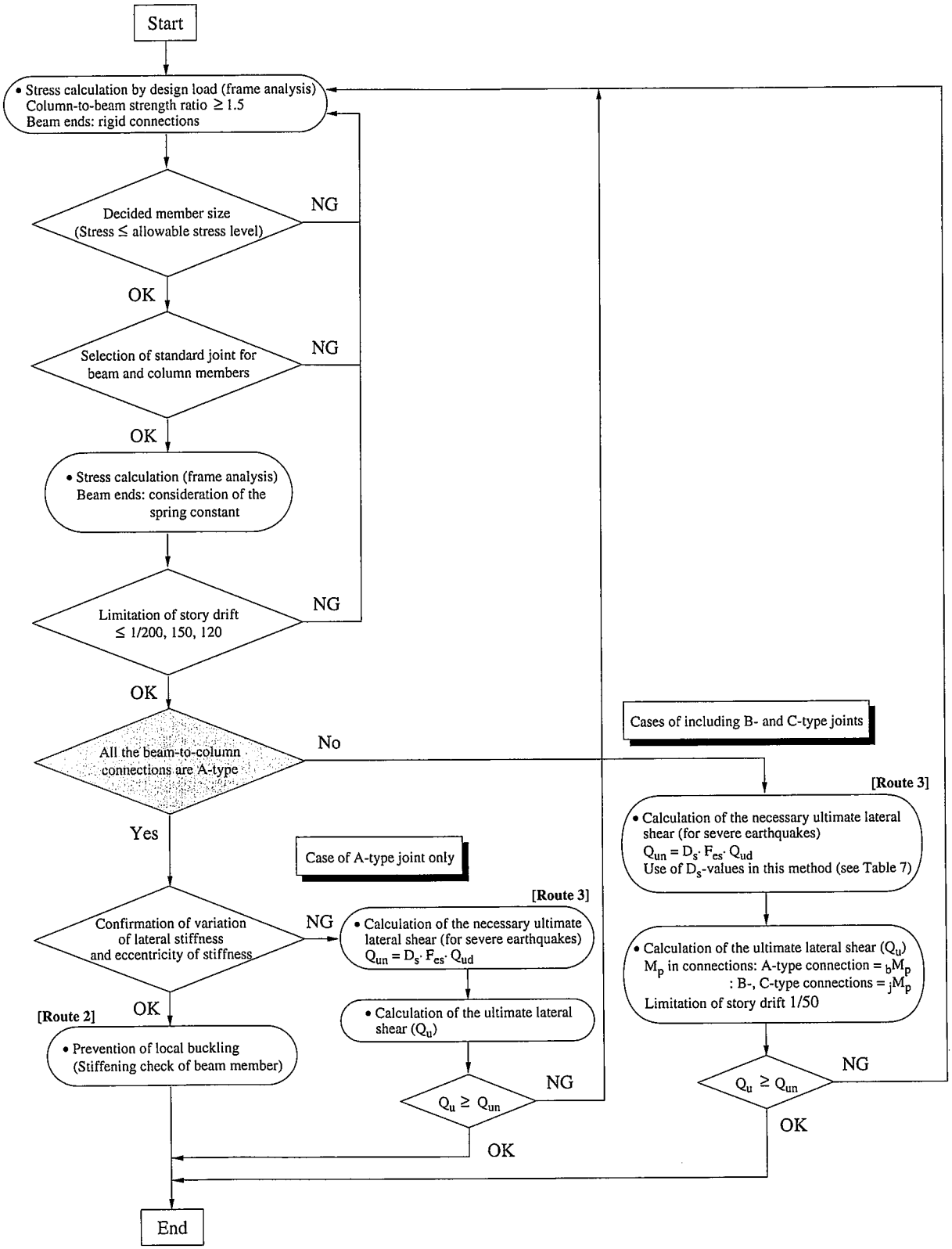

Fig. 15 Design flow

3.2.2 Story drift calculation

The stiffness of the beam-to-column connections is calculated based on the out-of-plane deformation on the tensile flange side, with the assumption that the compressed flanges of the beam is adequately rigid. Therefore, deformation in the connections can be expressed as the sum of the deformation ${}_c\delta$ of the square tube and the deformation ${}_t\delta$ of T-stub, using the deformation model[9] shown in **Fig. 16**. The tensile stiffness K in the joint of the square tube and T-stub is given in the following formula with the out-of-plane stiffness ${}_cK$ of the square tube and the stiffness ${}_tK$ of the T-stub.

$$1/K = 1/{}_cK + 1/{}_tK \quad \cdots\cdots (2)$$

Therefore, the spring constant in rotation at the beam ends necessary for computing the frame story drift is given as the rotating stiffness value at the beam ends corresponding to the beam height, using the tensile stiffness K in the above formula. This spring constant is also calculated in the above-mentioned joint standard design manual for every combination of columns and beams.

3.3 Ultimate strength

3.3.1 Classification in joint performances

This system classifies the joint performances into three types: A, B and C as shown in **Fig. 17**, according to the relationship between the beam strength and the joint strength. That is, an A-type joint can transmit the beam full plastic moment and also satisfy the conditions of the retained strength connection, in which the plastic deformation capability of the beam can be adequately forecast. The B-type joint can transmit the beam full plastic moment, but does not satisfy the conditions of the retained strength connection. The C-type has low strength in connections to the beam full plastic moment and in the seismic design level for severe earthquakes, and plastic deformation of connections become dominant. As a result, in the case of an A-type joint, the plastic moment of the beam ends in such a seismic design is given by the full plastic moment of the beam. In the case of B- and C-type connections, it is given by the plastic moment in the joint area determined by the smaller of the strength of T-stub connection and the local strength of column skins.

3.3.2 Structural coefficient (D_s-values)

For the necessary ultimate lateral shear calculation of framing using this system, the D_s-values[9] shown in **Table 7** are adopted for each joint type. The D_s-values are based on the following formula and the results of the cyclic loading test using the cruciform partial framing shown in Section 2.2.3.

$$D_s = \frac{1}{\sqrt{2\mu - 1}} \quad \mu\text{: plastic deformation ratio} \quad \cdots\cdots (3)$$

4. Fabrication and Construction of Hyper-Frame System

4.1 Steel frame quality control

For the steel frame fabrication and on-site construction using this system, steel frame quality control is performed in accordance with "the Hyper-Frame System Fabrication and Construction Manual[9]" made up Guidelines for fabrications, site construction, and TCBB inspection and clamping procedure.

4.2 Field applications

This system has been applied to six buildings. **Photo 2** is an example of beam-to-column connections. It is an office building with a total area of about 1,400 m² in 4 stories, and moment-resisting frames are used in both directions. As for the site construction of the columns and beams, the lower-flange-side T-stub is brought to the site, after being attached beforehand at a shop, and the upper-flange-side T-stub is loaded while temporarily attached to the beam at the site. **Photo 3** is an example of a column-column joint. The joint is a double shear friction bolt joint, and the joint between the lower columns and the splice plates uses ordinary high-strength bolts, while the joint between the upper columns and the splice plates uses TCBB 24.

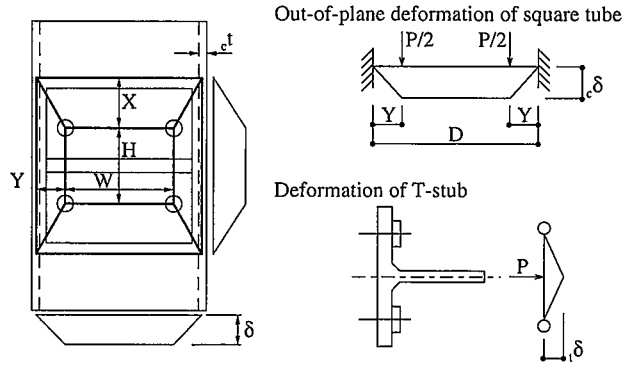

Fig. 16 Deformation models in connections

Table 7 Structural coefficient D_s-values of frame

Types of connctions	D_s-values
A-type	0.25
B-type	0.35
C-type	0.40

Note 1. Ranks of beams: Beams applicable to the connections targeted in this report are all A rank.

2. Decision of D_s-values: When several types of connections are mixed up in the framework, among the corresponding D_s-values, the maximum should be adopted as D_s-value. And the D_s-value is set up in each story.

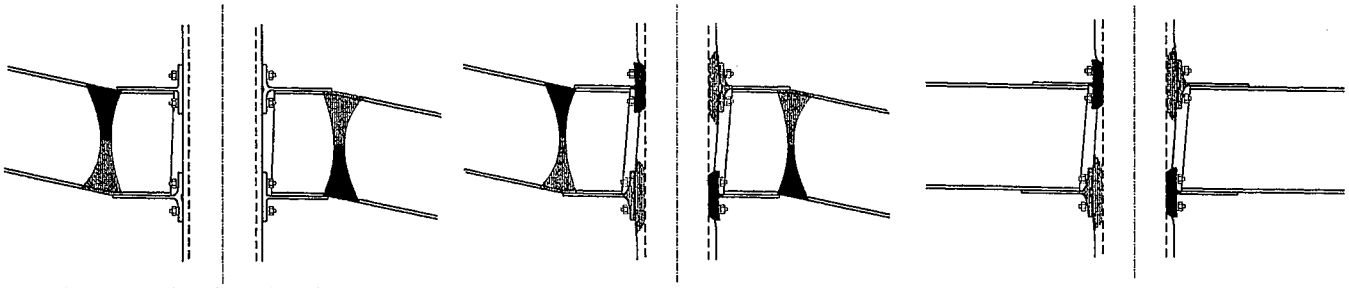

A-type: Plastic deformation of beams B-type: Plastic deformation of connections and beams C-type: Plastic deformation of connections

Fig. 17 Classification of joint performance

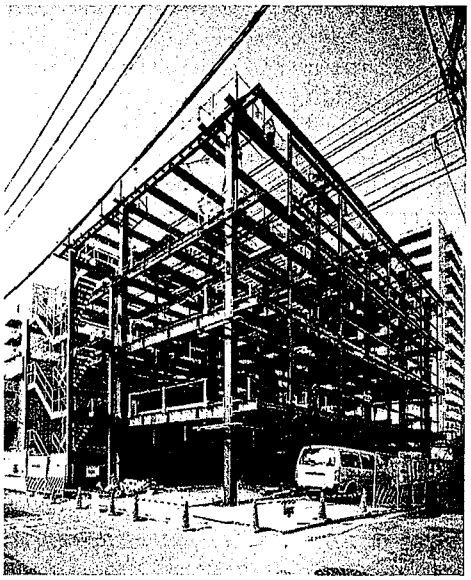

Photo 2 Application example of beam-to-column connections

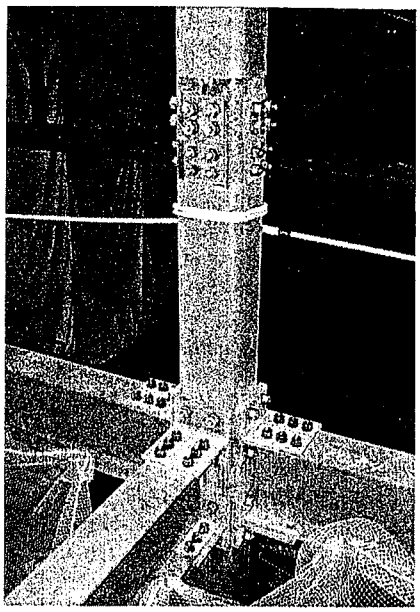

Photo 3 Application examples of column-to-column and beam-to-column connections

5. Conclusion

The application examples have confirmed the significant productivity improvements in fabrication, shortening of the work period, and good workability in on-site construction. It has been proved that this system is an effective method for ensuring the quality of steel frames mainly for low- to midrise buildings. Future development will widely expand the applied range of this system to steel frame building construction.

References

1) Uno, N.: Torque-Control, High-Strength Blind Bolt. Journal of Architecture and Building Science. 110 (1367), 60 (1995)
2) Takeuchi, I. et al.: Experimental Study on H-shaped Beam to Box Column Connections with Torque-Control Blind Bolts, Part 1 to 3. Summaries of Technical Papers of Annual Meeting, Hokkaido, 1995. 8, p.529
3) Uno, N., Furumi, K., Gojo, K.: Torque-Control Blind Bolt. The Building Letter. (365), 1(1997. 8)
4) AIJ: Standard for Limit State Design of Steel Structures (draft). 1990
5) Takagi, T. et al.: Experimental Study on H-shaped Beam to Box Column Connections Part 4. Summaries of Technical Papers of Annual Meeting, Hokkaido, 1995. 8, p.535
6) Shimura, Y., Nagata, M.: Non-weld Beam-to-Column Connections Using High-Strength Blind Bolts. Kenchiku Gijutsu. 142(1997. 4)
7) Nippon Steel Corporation: Hyper-Frame System Standard Design Manual. 1997. 6
8) Shimura, Y., Uno, N., Nagata, M.: Hyper-Frame System Blind Fastening System for Square Tube Columns. The Building Letter. (365), 4(1997. 8)
9) Nippon Steel Corporation: Hyper-Frame System Fabrication and Construction Manual. 1997. 6